Structural Studies of Polymer Blends by Solid-State NMR

HIROMICHI KUROSU[1] AND QUN CHEN[2]

[1]*Department of Human Life and Environment, Nara Women's University, Kitauoya-Nishimachi, Nara 630-8506, Japan*
[2]*Analytical Center and The Key Laboratory of Education Ministry for Optical and Magnetic Resonance Spectroscopy, East China Normal University, Shanghai 200062, P. R. China*

In this review, we introduce recent research works on polymer blends as studied by solid state NMR and focus on the miscibility and phase separation of polymer blends that are responsible for the improvement in their physical properties.

1. INTRODUCTION

It is well-known that most polymer blends are immiscible since the combinatorial entropy of mixing is small and the free volume contribution increases the free energy of mixing. Therefore, it is necessary to have specific intermolecular interactions which are responsible for miscibility, such as hydrogen bonding, dipole–dipole interaction, ion interactions etc. Since the physical properties of polymer blends are strongly influenced by the miscibility, there is much interest in studying miscibility and phase behaviour. A better understanding of miscibility and phase behaviour of polymer blends are essential for the development of blend materials. Polymer blends are of particular interest because of the practical motivation for producing new materials. The use of polymer blends to obtain materials with specific performance is widespread in manufacturing.

ANNUAL REPORTS ON NMR SPECTROSCOPY
VOLUME 52 ISSN 0066 4103
DOI 10.1016/S0066-4103(04)52004-5

Solid state NMR offers powerful tools for probing miscibility, phase separated structure and molecular motion in polymer blends and which may be beyond the resolution limits of conventional microscopic or thermal analysis. A large number of NMR works have been published and some of them were reviewed.[1,2] In this review, therefore, we introduce recent research works on polymer blends by solid state NMR and focus on the miscibility and phase separation of polymer blends that are responsible for the improvement in their physical properties.

2. MISCIBILITY

2.1. Relaxation measurements

In polymer blends, the ^{1}H spin-lattice relaxation times in the rotating ($T_{1\rho}{}^{H}$) and laboratory frames ($T_1{}^{H}$) obtained from high-resolution solid-state ^{13}C CP/MAS NMR are sensitive to the domain size of polymer blends through the process of proton spin diffusion. Proton spin diffusion is not a physical movement of protons, but is the equilibration process of non-equilibrium polarizations of spins at different local sites which occur through the mutual exchange of magnetization. The $T_{1\rho}{}^{H}$ is measured by employing a CP pulse sequence modified by adding a variable spin-locking pulse immediately after the ^{1}H $\pi/2$ pulse. The $T_1{}^{H}$ is measured from CP/MAS ^{13}C NMR using an inversion-recovery pulse sequence.

Chang *et al*. reported the miscibility of poly(vinylphenol) (PVPh) with poly(methyl methacrylate) (PMMA).[3] Figure 1 shows the ^{13}C CP/MAS spectra of pure PVPh, PMMA, PVPh-co-PMMA, PEG, and PVPh-*co*-PMMA/ poly(ethylene oxide) (PEO) blends of various compositions with peak assignments. VPh contents of PVPh-*co*-PMMA is 51 mol% and Mn of PEO is 20,000. The spin lattice relaxation time in the rotating frame ($T_{1\rho}{}^{H}$) was measured to examine the homogeneity of PVPh-*co*-PMMA/PEO blends on the molecular scale.

Table 1 summarizes those $T_{1\rho}{}^{H}$ values derived from the binary exponential analysis, indicating that the blend with high PVPh-*co*-PMMA content exhibits a single exponential. However, the biexponential decay gradually appears at higher PEO contents at 70 ppm. A semicrystalline polymer will have two proton spin lattice relaxations; the crystalline phase and the amorphous phase, attributed to the long and short relaxation components, respectively. According to Table 1, the amorphous $T_{1\rho}{}^{H}$ decreases with increasing PEO content in the blend. Meanwhile, a high $T_{1\rho}{}^{H}$ value for PVPh-*co*-PMMA/PEO = 80/20 blend, implies that the polymer mobility is retarded reflecting the more rigid character of the PVPh-*co*-PMMA. On the contrary, a decrease of the $T_{1\rho}{}^{H}$ value in the PEO rich region is associated with increased mobility of the amorphous PEO, related to the reduction of the intermolecular

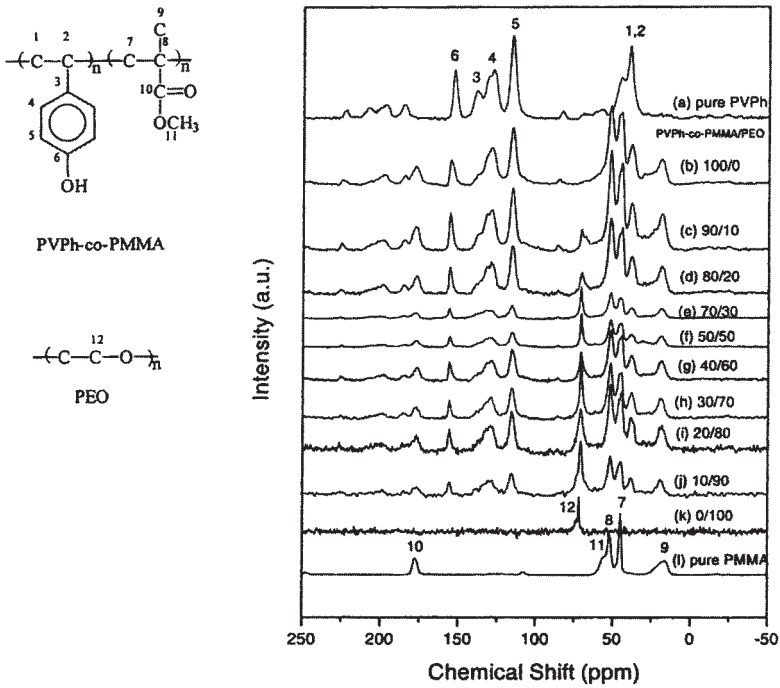

Fig. 1. ^{13}C CPMAS spectra at room temperature for pure PVPh, pure PMMA and various PVPh-*co*-PMMA/PEO blends: (a) pure PVPh; (b) 100/0; (c) 90/10; (d) 80/20; (e) 70/30; (f) 50/50; (g) 40/60; (h) 30/70; (i) 20/50; (j) 10/90; (k) 0/100; (l) pure PMMA. (Figures 1 and 9 in the original literature: S. W. Kuo and F. C. Chang, *Macromolecules*, 2001, **34**, 4089.)

Table 1. $T_{1\rho}{}^{H}$ (ms) values of pure PVPh and various PVPh-*co*-PMMA/PEO blend compositions

Blend composition	115 ppm	70 ppm	
Pure PVPh	7.24		
PVPh-*co*-PMMA/PEO			
100/0	12.08		
80/20	5.21	1.48	
40/60	4.30	1.38	
20/80	4.77	0.95	3.93
0/100		0.08	7.84

hydrogen bonding strength. An increasing amount of the long relaxation component with increasing PEO suggests the existence of a more crystalline PEO phase in the blend.

Table 1 also shows that both pure PVP and PVPh-*co*-PMMA/PEO blends exhibit only single-exponential relaxation through out all of the blends at

115 ppm, indicating good miscibility and dynamic homogeneity in the PVPh-co-PMMA phase. The maximum diffusive path length L can be estimated using the approximate Eq. (1).[4–6]

$$L = (6DT)^{1/2} \tag{1}$$

A typical value of D is 10^{-16} m^2 s^{-1}. For $T_{1\rho}{}^{H}$ of 5 ms, the dimensions of these PVPh-*co*-PMMA/PEO blends are below 2–3 nm in the amorphous phase. Interestingly, the $T_{1\rho}{}^{H}$ has a minimum value for the PVPh-*co*-PMMA = 40/60 blend showing that the overall chain mobility is maximal at this composition. This observation agrees with the earlier result concerning hydroxyl group association obtained by FTIR and solid-state NMR. In addition, all of the blends show a shorter $T_{1\rho}{}^{H}$ than that of the pure PVPh-*co*-PMMA implying that the PVPh-*co*-PMMA mobility also increases with the increase of PEO content.

The miscibility of poly(methyl acrylate) (PMAA, Mw = 150,000)/PVAc (Mw = 167,000) blends at various mixing ratios was investigated by both $T_1{}^{H}$ and $T_{1\rho}{}^{H}$ measurements.[7] ^{13}C CP/MAS NMR spectra of PMAA, PVAc and the PMAA/PVAc blends are shown in Fig. 2. Figure 3 shows the plots of the ^1H spin-lattice relaxation times in the laboratory ($T_1{}^{H}$, A) and in the rotating ($T_{1\rho}{}^{H}$, B) frames against the molar ratio of PMAA (χ_{PMAA}). The ^1H relaxation times from the CH_2 (○) and OCH (▲) carbons for PMAA and PVAc, respectively, can be observed because these two carbons are observed separately even in the blends (Fig. 2), so that it is possible to obtain each ^1H relaxation time for PMAA or PVAc in the blends independently.

Figure 3A shows that both the original $T_1{}^{H}$ values of pure PMAA and pure PVAc alter in the blends and the obtained $T_1{}^{H}$ values of PMAA are in excellent agreement with those of PVAc. This indicates that the complete averaging of the $T_1{}^{H}$ rates by ^1H spin diffusion, suggesting that PMAA and PVAc are in close proximity with each other and the PMAA/PVAc blends are homogeneous on a scale of 20–50 nm for all compositions. Similarly, Fig. 3B shows that the $T_{1\rho}{}^{H}$ values of PMAA in the PMAA-rich/PVAc blends, which are the PMAA/PVAc = 3/1, 2/1, and 1/1 blends, are fully consistent with those of PVAc. For the PMAA/PVAc-rich blends, which are the PMAA/PVAc = 1/2 and 1/3 blends, however, the $T_{1\rho}{}^{H}$ values of PMAA are different from those of PVAc, although the values of PMAA or PVAc alter toward each other and become close from those of pure ones. This exhibits that the partially averaging of $T_{1\rho}{}^{H}$ rates by ^1H spin diffusion occurs in the PMAA/PVAc-rich blends. These results show that the PMAA-rich/PVAc blends are homogeneous on a scale of 2–5 nm as well as 20–50 nm, but the PMAA/PVAc-rich blends are inhomogeneous on the scale.

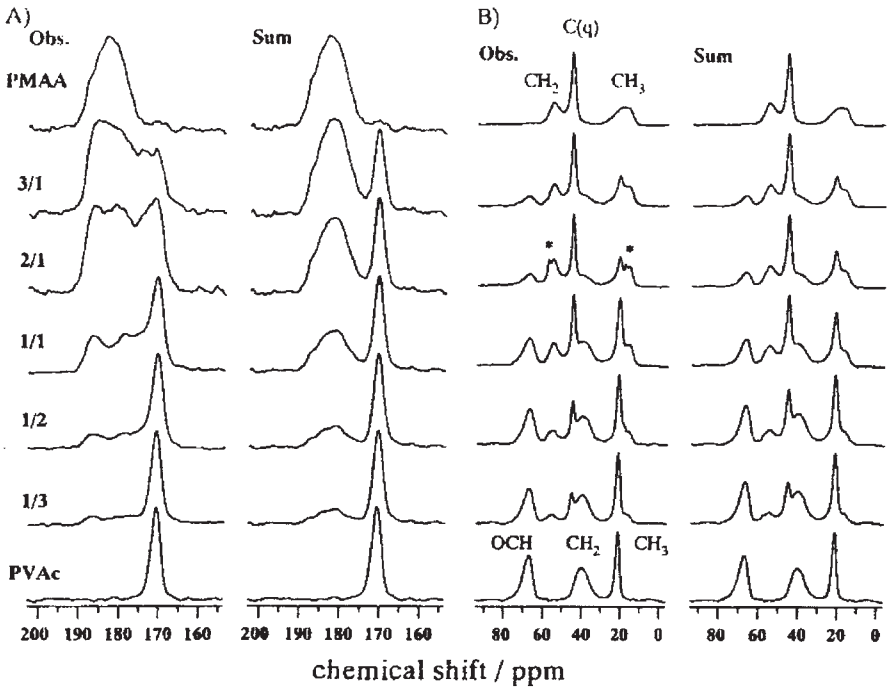

Fig. 2. Observed CP/MAS ^{13}C NMR spectra of PMAA, PVAc, and the PMAA/PVAc blends: (A) carboxyl regions of PMAA and carbonyl regions of PVAc. (B) Aliphatic region. The sum of the ^{13}C NMR spectra of pure PMAA and pure PVAc at the respective molar unit ratio is also depicted on the right of the observed spectra. (Figure 1 in the original literature: A. Asano, M. Eguchi, M. Shimizu and T. Kurotsu, *Macromolecules*, 2003, **25**, 8819.)

If the ^{1}H spin diffusion occurs entirely during a period less than the shortest ^{1}H relaxation time among the mixed polymers, the ^{1}H relaxation rate is averaged by ^{1}H mole fraction as follows:

$$1/T_1{}^{Ave} = f_{PMAA} \times 1/T_1{}^{PMAA} + (1 - f_{PMAA}) \times 1/T_1{}^{PVAc} \qquad (2)$$

where $T_1{}^{Ave}$ is the averaged ^{1}H relaxation time and f_{PMAA} the ^{1}H mole fraction of PMAA in the respective blend. $T_1{}^{PMAA}$ and $T_1{}^{PVAc}$ are the ^{1}H relaxation times for pure PMAA and PVAc, respectively. In a case of no significant change of molecular motion between the pure and the mixed states, the observed ^{1}H relaxation times for the blends are equal to the calculated values obtained from Eq. (2).

The solid lines in Fig. 4A and B represent the calculated values from Eq. (2). The observed $T_1{}^{H}$ values are in good agreement with the estimated values. The observed $T_{1\rho}{}^{H}$ values for PMAA-rich blends are also in good agreement with the calculated ones. These agreements indicate that the molecular motions

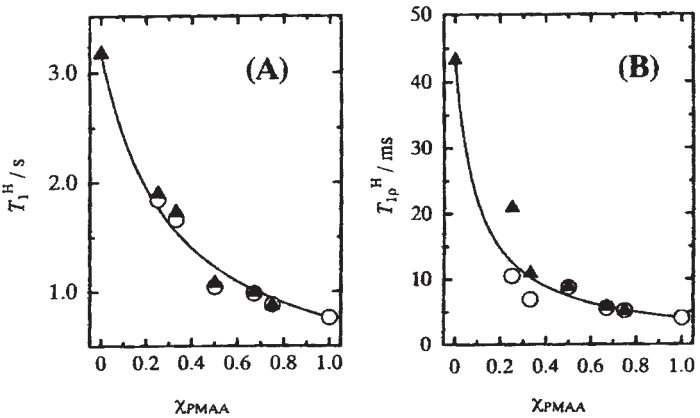

Fig. 3. Observed ^{1}H spin-lattice relaxation times in the laboratory (T_1^H, A) and in the rotating ($T_{1\rho}^H$, B) frames against the molar unit ratio of PMAA/PVAc blends (χ_{PMAA}): O, CH_2 carbon of PMAA; ▲, OCH carbon of PVAc. Each solid line represents the calculated curve from Eq. (2). (Figure 3 in the original literature: A. Asano, M. Eguchi, M. Shimizu and T. Kurotsu, *Macromolecules*, 2003, **25**, 8819.)

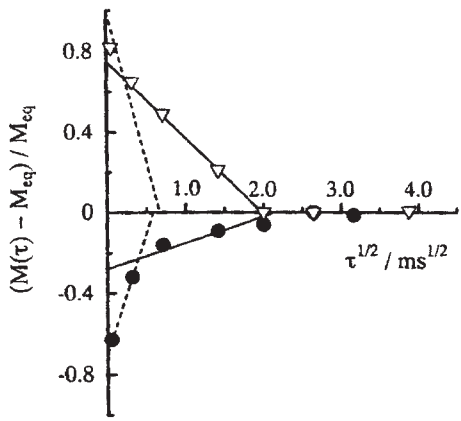

Fig. 4. Plots of ^{1}H normalized magnetization change (●, C(q) signal of PMAA; ▽, CH_3 signal of PVAc) vs. square root of ^{1}H spin-diffusion time $\tau^{1/2}$ for the PMAA/PVAc = 1/1 blend. Solid straight lines are drawn without the initial point to determine the intercept time te. Broken lines are drawn through the initial and the second data points. Meq represents the quasi-equilibrium magnetization after long mixing period but much shorter than T_1^H. (Figure 4 in the original literature: A. Asano, M. Eguchi, M. Shimizu and T. Kurotsu, *Macromolecules*, 2003, **25**, 8819.)

of both polymers in the blends are not changed drastically with each other compared with those found before mixing, and the fast ^{1}H spin diffusion is not hindered by the molecular motions. These results are reasonable by taking account of the high Tg for these blends.

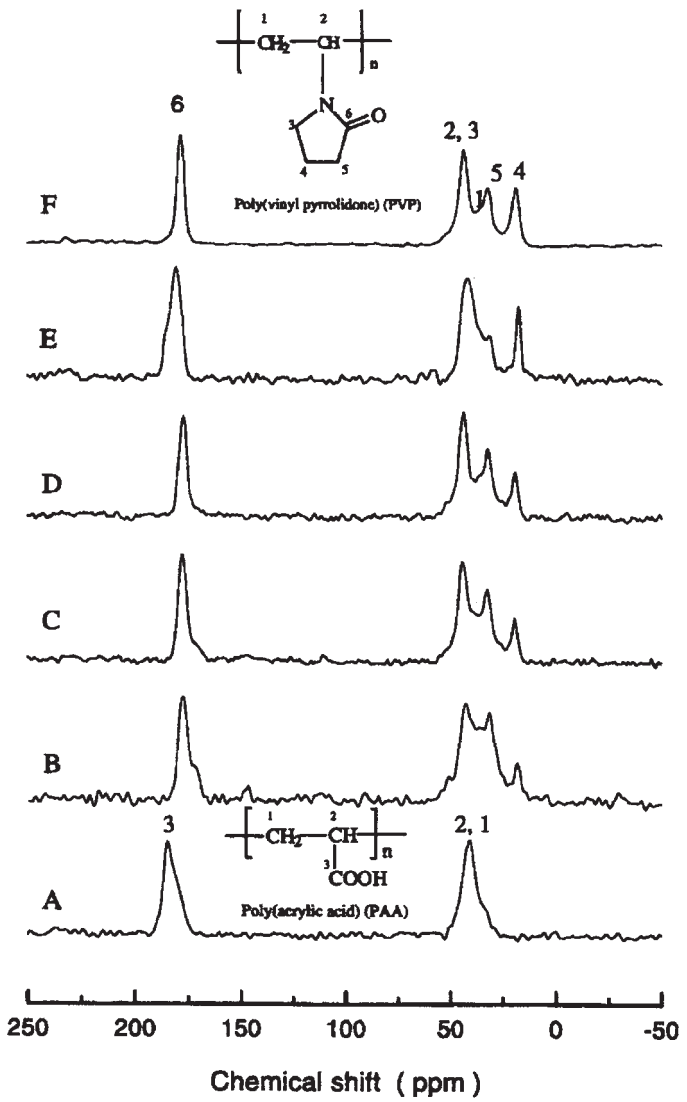

Fig. 5. ^{13}C CP/MAS spectra of the PAA/PVP blends: (A) 100/0; (B) 60/40; (C) 40/60, (D) 22/78; (E) complex (1/1); (F) 0/100. (Figure 6 in the original literature: C. Lau and Y. Mi, *Polymer*, 2002, **43**, 823.)

The miscibility of poly(acrylic acid) (PAA) and poly(vinyl pyrrolidone) (PVP) blends and complex was investigated by relaxation measurements.[8] Figure 5 shows ^{13}C CP/MAS spectra of the PAA/PVP blends, PAA, PVP and complex. In the $T_1{}^H$ experiment, the resonance intensities of all the samples were obtained with a series of different delay times based on the inversion

Table 2. The mean value of T_1^H and $T_{1\rho}^H$ for PAA/PVP system and their standard deviation

	Sample	wt/wt	mol/mol	T_1^H (s)	$\sigma\ T_1^H$	$T_{1\rho}^H$ (ms)	$\sigma\ T_{1\rho}^H$
	PAA	100/0		2.59	0.01	6.36	0.01
PAA/PVP	Blend	60/40	2/1	1.77	0.07	9.34	0.28
PAA/PVP	Blend	40/60	1/1	1.79	0.07	9.06	0.23
PAA/PVP	Blend	22/78	1/2	2.01	0.12	9.45	0.52
	PVA	0/100		1.83	0.03	15.21	0.43
PAA/PVP	Complex	49/51	1.48/1	2.36	0.15	5.46	0.22

recovery mode. The intensity of the resonance carbons can be described by the following exponential model,

$$\ln\left[\frac{M_e - M_\tau}{2M_e}\right] = \frac{-\tau}{T_1^H} \tag{3}$$

The mean value of the T_1^Hs for each sample was calculated. The calculated mean values of T_1^Hs and the standard deviations are presented in Table 2. It is seen, from Table 2, that the standard deviation in both blends and complex is negligibly small. This indicates that the spin-diffusion among all protons in the blends and the complex can average out the whole relaxation process and hence the domain size of these samples is smaller than the spin-diffusion path length within the time frame of T_1^H. From the obtained value of T_1^H and using the Eq. (1) with 10^{-16} m^2 s^{-1}, it is believed that the PAA/PVP blends are intimately mixed on the T_1^H measurement scale of 32–39 nm.

The miscibility of the blends and complex can be probed at even smaller scale by carrying out the $T_{1\rho}^H$ measurement, in which the relaxation time, $T_{1\rho}^H$, was determined by monitoring the decay in carbon signal intensities as a function of delay time. All the resonance peaks show a single-exponential decay and the logarithmic plot of ^{13}C resonance intensity M_τ vs. delay time τ for the selected carbon (33 ppm) of pure PVP, PAA/PVP blend (1/1), and complex. Furthermore, it can be seen from Table 2 that the standard deviation can be ignored and the $T_{1\rho}^H$ values obtained for each sample can be considered to be the same. All these imply that all of the blends and the complex are intimately mixed on the $T_{1\rho}^H$ measurement scale. The homogeneity data are accurate down to the scale of 2 nm for the blends and 1.5 nm for the complex.

Miscibility of amorphous poly(benzyl methacrylate) (PBzMA) and semicrystalline poly(ethylene oxide) (PEO) blends were investigated by solid state ^{13}C NMR.[9] Figure 6 shows the ^{13}C CP/MAS NMR spectrum of the PBzMA/PEO blend in 80/20 composition and the ^{13}C CP/MAS NMR spectra of various compositions are shown in Fig. 7. The logarithmic plots of ^{13}C

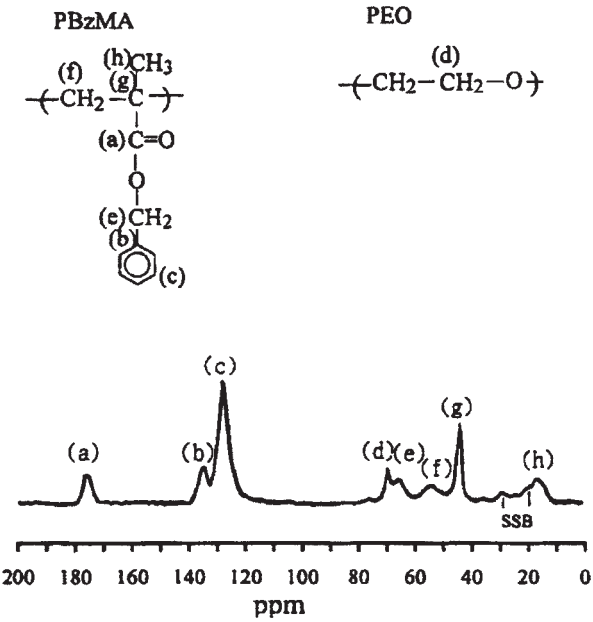

Fig. 6. ^{13}C CP/MAS NMR spectrum of the PBzMA/PEO blend in 80/20 composition. SSB denotes spinning side-band. (Figure 1 in the original literature: R.-H. Lin, E. M. Woo and J. C. Chiang, 2001, *Polymer*, **42**, 4289.)

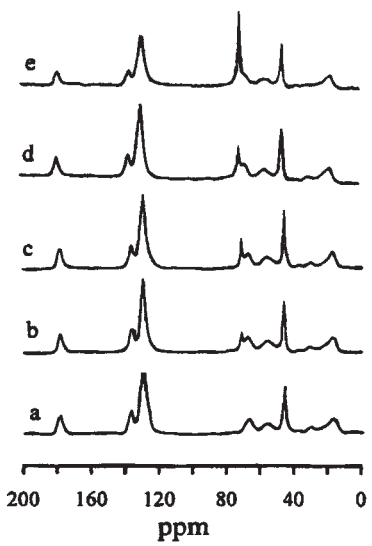

Fig. 7. ^{13}C CP/MAS NMR spectra of the PBzMA/PEO blends in various compositions: (a) 100/0, (b) 90/10, (c) 80/20, (d) 50/50 and (e) 30/70. (Figure 2 in the original literature: R.-H. Lin, E. M. Woo and J. C. Chiang, *Polymer*, 2001, **42**, 4289.)

magnetization intensity versus spin-lock time using a 1 ms contact time for neat samples of PBzMA and PEO. Neat PBzMA is characterized by single-exponential $T_{1\rho}^{H}$ relaxation behaviour, consistent with results usually observed on the amorphous polymer. Neat PEO also exhibits a single-exponential $T_{1\rho}^{H}$ relaxation behaviour using a 1 ms contact time. However, it displays double-exponential $T_{1\rho}^{H}$ relaxation behaviour if we use a 0.1 ms contact time, indicating that PEO contains dual morphologies. Essentially, PEO is a well-known semicrystalline polymer containing an amorphous phase and a crystalline phase. It should be noted that crystalline PEO, which has a very short $T_{1\rho}^{H}$, cannot be detected using a 1 ms contact time. The fitted values of $T_{1\rho}^{H}$ are 7.74 ms for neat PBzMA, and 2.72 and 0.2 ms for neat PEO, as listed in Table 3. The short $T_{1\rho}^{H}$ (0.2 ms) can be associated with the protons of the crystalline parts of PEO, and long $T_{1\rho}^{H}$ (2.72 ms) is contributed by the amorphous phase of PEO.[10] $T_{1\rho}^{H}$ for the PBzMA, PEO and PBzMA/PEO blends are listed in Table 3. PBzMA components in the blends were observed to exhibit single-exponential $T_{1\rho}^{H}$ relaxation behaviour through all the cases of different compositions, indicating that the PBzMA component always exhibits a homogenous phase within the blends at various compositions. This homogenous phase is not pure PBzMA, because the values of $T_{1\rho}^{H}$ for the PBzMA component are not identical to that in the neat PBzMA system (7.74 ms). In spite of the PEO content in the blend, the PBzMA component always predominates in the miscible amorphous phase because the $T_{1\rho}^{H}$ values in this phase are always closer to that of the neat PBzMA component (7.74 ms) and far way from that of the neat amorphous PEO component (2.72 ms). That indicates a miscible homogenous PBzMA-rich phase at a nanoscale level in the blends. Besides, those values of $T_{1\rho}^{H}$ for the PBzMA component slightly decrease (approaching the value of neat PEO) as the PEO component in the blend increases, suggesting that the PEO component in this miscible homogenous phase is presumably enhanced in a gradual way. For each blend the $T_{1\rho}^{H}$ values for PBzMA (6.27, 6.03, 5.72, and 5.34 ms) are eventually identical to the long $T_{1\rho}^{H}$ of the PEO component. This indicates

Table 3. $T_{1\rho}^{H}$ for the PBzMA, PEO and PBzMA/PEO blends (contact time: 1 ms)

PBzMA/PEO Blend (wt/wt)	PBzMA component $T_{1\rho}^{H}$ (ms)	PEO component $T_{1\rho}^{H}$ (ms)		
100/0	7.74	–		
90/10	6.27	6.33	–	
80/20	6.03	6.02	2.76	
50/50	5.72	5.70	2.77	
30/70	5.34	5.40	2.73	
0/100	–		2.72	0.2[a]

[a]Obtained using a contact time of 0.1 ms.

those miscible homogenous phases with PBzMA and PEO chains mixed at the molecular level.

However, double-exponential $T_{1\rho}{}^{H}$ relaxation behaviour of the PEO component in various compositions of blends except 90/10 (PBzMA/PEO) were observed and the long $T_{1\rho}{}^{H}$ of the PEO component was virtually the same as the $T_{1\rho}{}^{H}$ of PBzMA in the PBzMA-rich domain for each composition of blend, whereas all the short $T_{1\rho}{}^{H}$ of the PEO component in each blend were of the same value (about 2.75 ms) and identical with that of the amorphous phase of neat PEO. This suggests that the amorphous PEO component in each blend is distributed unevenly into two separated phase domains on a $T_{1\rho}{}^{H}$ relaxation scale. The PEO component in the blend of 90/10 (PBzMA/PEO) composition still exhibits a single-exponential $T_{1\rho}{}^{H}$ relaxation behaviour (6.33 ms). This single value of $T_{1\rho}{}^{H}$ for the PEO component is virtually the same as that of the PBzMA component, indicating that this blend is completely homogenous PBzMA-rich phase without constrained PEO and crystalline PEO. Thus, the non-crystallizable portion is referred to the 'constrained PEO' region. This inference illustrates that only one phase is present for this blend (90/10), which will be verified later in more detail.

The miscibility of poly(ethyl oxazoline) (PEOx)/poly(4-vinylphenol) (PVPh) blends were investigated by the solid state NMR.[11] Figure 8 shows the ^{13}C CP/MAS spectra of the PEOx/PVPh blends. To obtain information about the scale of miscibility and phase structure of the PEOx/PVPh blends, dynamic relaxation experiments were conducted, which include the measurements of the $T_1{}^{H}$, and $T_{1\rho}{}^{H}$. In $T_1{}^{H}$ experiment, peak intensities of PEOx, PVPh and their blends change exponentially as a function of delay time (τ). From the slopes of the plots, $T_1{}^{H}$s were obtained, and the results of $T_1{}^{H}$ for PEOx, PVPh and their blends are summarized in Table 4. Intermediate values of $T_1{}^{H}$ were obtained for the blends compared to those of the two pure components. These results indicate that fast spin diffusion occurrs among all of the protons in these blends, which averages out the entire relaxation process. Therefore, the blends are homogenous on the scale where the spin diffusion occurs within the time-frame of $T_1{}^{H}$, and the mixing scale can be estimated using the one-dimensional diffusion equation for the average diffusive path length as shown in Eq. (1).

$T_{1\rho}{}^{H}$ was measured to examine homogeneity of the PEOx/PVPh blends at the molecular level. In this measurement, the intensities of carbon peaks of PEOx, PVPh and their blends display single exponential decays as a function of delay time. Values of calculated $T_{1\rho}{}^{H}$ are summarized in Table 4. A single $T_{1\rho}{}^{H}$ value was obtained for both pure components and blends and the values of the blends were larger than those of the two pure components, indicating strong hydrogen bonding between the two components, that restricts the segmental motion of the polymer chains and cause the relaxation times of the blends to be longer than those of the pure components. Thus, the

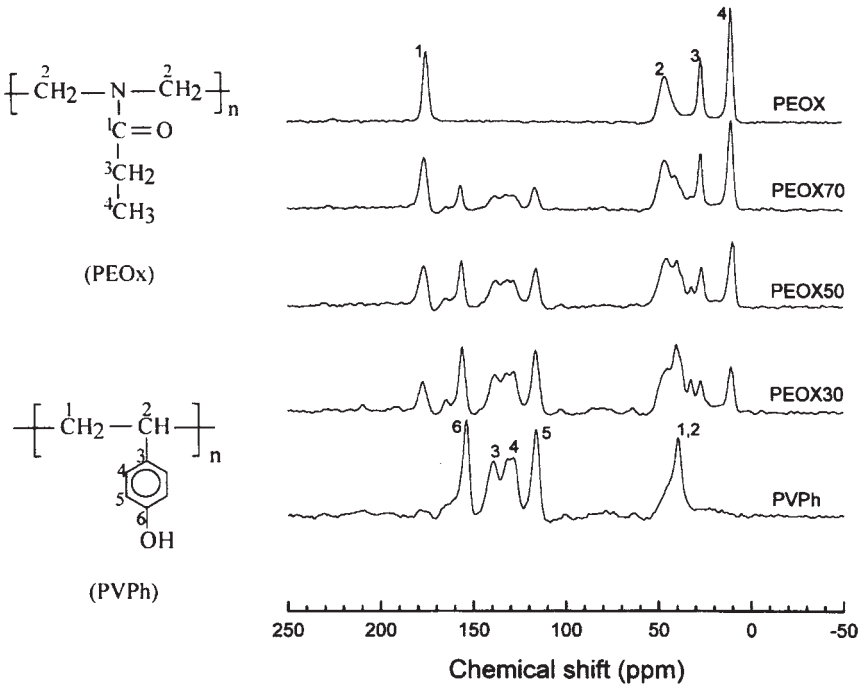

Fig. 8. ^{13}C CP/MAS NMR spectra of the PEOx/PVPh blends in various compositions. (Figure 4 in the original literature: J. Wang, M. K. Cheung and Y. Mi, *Polymer*, 2002, **42**, 2077.)

Table 4. $T_1{}^H$ and $T_{1\rho}{}^H$ values for PEOx, PVPh and their blends (the accuracy of the measurements is ±15%)

	$T_1{}^H$ (s)		$T_{1\rho}{}^H$ (ms)	
PEOx/PVPh	PEOx C-3	PVPh C-5	PEOx C-3	PVPh C-5
100/0	2.76	–	7.16	–
70/30	2.62	2.65	8.57	8.06
50/50	2.39	2.35	8.74	8.90
30/70	2.04	2.27	8.59	8.10
0/100	–	1.32	–	6.79

blends are homogeneous on the $T_{1\rho}{}^H$ sensitive scale of 2–3 nm according to Eq. (1).

Miscibility of poly(4-vinylpyridibe) (P4VP) and PVPh is investigated by solid state NMR.[12] ^{13}C CP/MAS NMR spectra of P4VP/PVPh blends in various composition are shown in Fig. 9. To obtain information about the

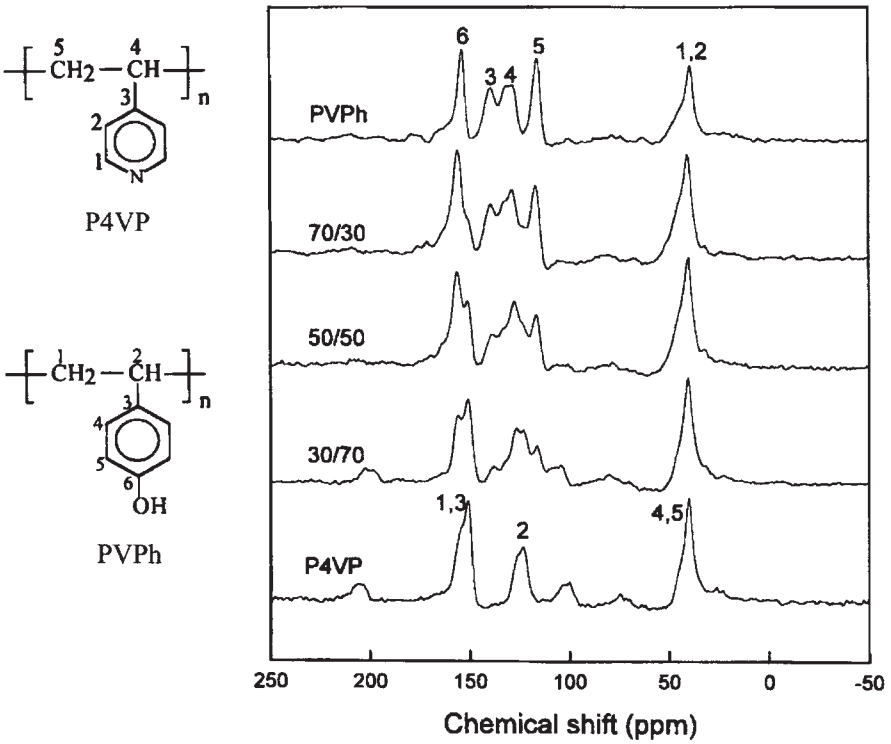

Fig. 9. ^{13}C CP/MAS NMR spectra of the P4VP/PVPh blends in various composition. (Figure 4 in the original literature: J. Wang, M. K. Cheung and Y. Mi, *Polymer*, 2001, **42**, 3087.)

scale of miscibility and phase structure of the P4VP/PVPh blends, relaxation time measurements were performed, which include the measurements of T_1^H, and $T_{1\rho}^H$. The experimental data can be fitted to a single exponential decay function, and from the slopes of the plots, T_1^H values can be obtained. It is found that single T_1^H decays are obtained for all blends, which indicates that fast spin diffusion occurred among all protons in these blends in the entire relaxation process. In addition, it is also found that the T_1^H values of the blends are shorter than those of the pure components, which indicates that the intermolecular interactions are stronger than the intra-molecular self-associations. This specific interaction is analysed to be hydrogen bonding between the nitrogen in the pyridine ring of P4VP and the hydroxyl groups in PVPh. The mixing scale can be estimated using Eq. (1). On the basis of T_1^H, it is believed that the two polymers are intimately mixed on a scale of less than 60–80 nm. Since such mixing level reflects the sum of domain A plus domain B of the blends, the domain size of a constituent domain is less than 40 nm.

Table 5. T_1^H (s) and $T_{1\rho}^H$ (ms) values of P4VP/PVPh blends at 300 K

P4VP/PVPh	T_1^H (s)		$T_{1\rho}^H$ (ms)	
	P4VP C-4,5	PVPh C-5	P4VP C-4,5	PVPh C-5
100/0	1.55	–	6.79	–
70/30	1.20	0.93	7.80	10.71
50/50	1.10	0.97	8.40	9.40
30/70	1.08	0.94	8.69	9.10
0/100	–	1.32	–	6.80

The spin-lattice relaxation time in the rotating frame $T_{1\rho}^H$ was measured to examine homogeneity of the P4VP/PVPh blends at the molecular level. It is found that the experimental data can be fitted to a single exponential decay function, and the slope gives the $T_{1\rho}^H$ value. The $T_{1\rho}^H$ values of the P4VP/PVPh blends (30/70, 50/50, 70/30) are longer than those of the two pure components as listed in Table 5. The likely molecular motions in this frequency range are those due to the pendent groups of P4VP and PVPh. Since strong inter-molecular hydrogen bonding hinders the motion of the pendent groups, the $T_{1\rho}^H$ is longer for the blends.[13–15] These imply that all the blends are homogeneous on the $T_{1\rho}^H$ sensitive scale.

By measuring $T_{1\rho}^H$, Chu *et al.*[16] studied the morphology and molecular dynamics of poly(amide-6) (PA6)/poly(2,6-dimethyl-1,4-phenylene oxide) (PPO) blends compatiblized with styrene maleic anhydride (SMA). SEM photomicrograph measurements demonstrate that the domain size of PA6/PPO blend (30/70 by weight) is reduced greatly with increasing SMA content. PA6, which remains semicrystalline in the blend samples, exhibits biexponential $T_{1\rho}^H$ relaxation behaviour. The long $T_{1\rho}^H$ value is attributed to the crystalline component, while the short one to the amorphous component. PPO, on the other hand, shows only a single $T_{1\rho}^H$ value. For all of the samples studied in the work, the $T_{1\rho}^H$s of the different components are not averaged by spin-diffusion to a common value, indicating the samples are phase separated at the length scale of several tens of Å. It is demonstrated that with increasing SMA content, the crystalline fraction of PA6 decreases steadily, due to the formation of SMA-g-PA6 segments. The mobility of amorphous PA and PPO is found to be enhanced with an increase of SMA. Mechanical properties, including tensile strength, tensile elongation and impact strength of the blends before and after annealing are correlated with $T_{1\rho}^H$ values. It is demonstrated that mechanical properties are sensitive to the molecular structures and dynamics take place within the range of several tens of Å.

Blends of polycaprolactone (PCL) with polyvinylalcohol (PVA) were studied by De Kesel *et al.*[17] Both constituent polymers are semicrystalline at the studying temperature. T_1^H is directly and indirectly measured by using

^{1}H wide-line and ^{13}C CP/MAS NMR techniques respectively. Both constituent polymers are found to exhibit same $T_1{}^{H}$ value, which is dependent on the blend composition. Such a result indicates the blends are compatible at the T_1 scale, namely 60–90 nm in this case.

Nakano *et al.*[18] reported a ^{13}C CP/MAS NMR study on poly(L-Alanine) (PLA)/Polyglycine (PG) blends. The comparison between the ^{13}C CP/MAS spectra of the blends and those of the parent polymers discloses that upon blending, new conformations of PLA and PG are formed, which is closely related to the presence of intermolecular hydrogen-bonding interactions. $T_{1\rho}{}^{H}$ measurements demonstrate that the major parts of PG and PLA in the blends, which are in 3_1-helix and α-helix conformation forms respectively, are phase separated. On the other hand, the β-sheet forms of PG and PLA, which are newly formed upon blending, exhibit similar $T_{1\rho}{}^{H}$ values, demonstrating that these two parts are miscible at the scale of 3–4 nm.

A solid-state ^{13}C NMR study of the intermolecular hydrogen bonding formation in a blend of phenolic resin and poly(hydroxyl ether) of bisphenol A was reported by Wu *et al.*[19] The presence of a single glass transition temperature for all of the blend samples with different composition as disclosed by the DSC measurements demonstrates that the blends are thermodynamically miscible. The solid state NMR parameters, including chemical shift, efficiency of cross-polarization and $T_{1\rho}{}^{H}$, confirm the presence of more free OH groups when one of the polymers is the minor component.

Hill *et al.*[20] studied the miscibility and hydrogen-bonding interactions in blends of poly(4-vinylphenol) (PVPh) and Poly(2-ethoxyethyl methacrylate) (PEEMA) by employing DSC, infrared spectroscopy (IR) and solid state NMR techniques. Figure 10 shows the ^{13}C CP/MAS signal of the carbonyl group of PEEMA as a function of blend composition. The signal of the blend samples apparently consists of two peaks, comparing with that of the neat PEEMA sample. The peak at the high frequency side is attributed to the hydrogen-bonded carbonyl groups, while the low frequency peak to the free carbonyl groups. The enhancement ratios of cross-polarization and the $T_{1\rho}{}^{H}$s for these two carbonyl peaks are almost equal to each other. This means that the relative peak intensities shown in Fig. 11 are quantitative. By analyzing the carbonyl signal, it is found that the fraction of hydrogen-bonded carbonyl groups decreases steadily with increasing the weight content of PEEMA, agreeing well with those obtained from the IR analyses. Similar results are also observed for the signal of phenolic carbon of PVPh, indicating that both the signals of carbonyl carbons and the phenolic carbons can be employed in quantitative determination of the fraction of intermolecular hydrogen-bonding. $T_{1\rho}{}^{H}$s of the blends are measured by ^{1}H wide-line NMR as well as ^{13}C CP/MAS NMR techniques. It is found that both components exhibit the same $T_{1\rho}{}^{H}$, the value of which depends on the blend composition. This result agrees well with those of DSC measurements,

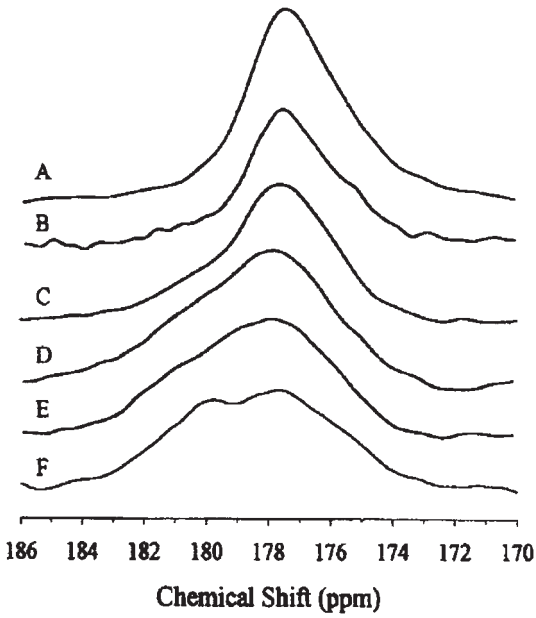

Fig. 10. ^{13}C CP/MAS spectra for the C=O resonance in the blends: (A) 100% PEEMA, (B) 85% PEEMA, (C) 75% PEEMA, (D) 55% PEEMA, (E) 45% PEEMA, (F) 30% PEEMA. (Figure 8 in original literature: D. J. T. Hill, A. K. Whittaker and K. W. Wong, *Macromolecules*, 1999, **32**, 5285.)

demonstrating that the blends are homogeneous. The scale of homogeneity is estimated to be about 2 nm from the value of $T_{1\rho}{}^{H}$.

Wang *et al*. studied the structure and dynamics of poly(aspartic acid) sodium (PAANa)/poly(vinyl alcohol) (PVA) blends by ^{13}C CP/MAS and ^{23}Na NMR spectrsocpy.[21,22] By comparing the ^{13}C CP/MAS spectra of the blends and the neat polymers, it is found that upon blending a new carbonyl peak appears at the high frequency side of the original carbonyl signal. This new peak is assigned to the carboxyl groups of the side chain of PAANa forming intermolecular hydrogen-bonds with the hydroxyl groups of PVA. The formation of intermolecular hydrogen-bonds is also evidenced by the intensity changes of the CH carbon of PVA upon blending. $T_1{}^{H}$ and $T_{1\rho}{}^{H}$ measurements via ^{13}C detection show that the miscibility of the blends is highly composition dependent, although certain amount of inter-polymer hydrogen-bonds exists. The miscibility of PAANa/PVA blend with a molar ratio of 1/1 is turned out to be the highest. This conclusion is supported by the results of the ^{23}Na MAS NMR spectra shown in Fig. 11. There are two peaks in ^{23}Na MAS spectrum of neat PAANa, which are corresponding to the isolated ^{23}Na (7 ppm) and associated ^{23}Na (−16 ppm), respectively. It is evident that in the spectrum of 1/1 blend, the peak of isolated ^{23}Na

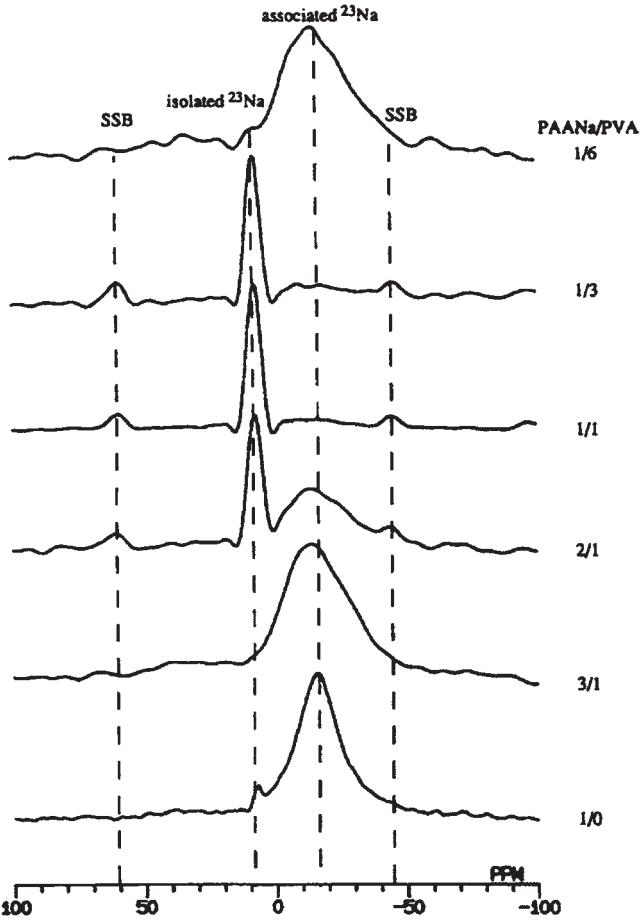

Fig. 11. ^{23}Na MAS NMR spectra of PAANa/PVA blends with various compositions at 25°C. (Figure 4 in original literature: P. Wang and I. J. Ando, *Mol. Struct.*, 1999, **508**, 97.)

exhibits highest relative intensity, indicating enrichment of the inter-polymer hydrogen-bonding interaction which leads to a reduction of the possibility of COO^- and Na^+ association.

A series of polymer blends with inter-polymer specific interactions were studied by Mi *et al.* by using DSC, IR, and ^{13}C CP/MAS NMR techniques.[13,23–25] $T_1{}^H$, $T_{1\rho}{}^H$ and the cross-polarization transfer constant (T_{CH}) measurements as well as the spectral feature analyses were carried out to investigate the miscibility and inter-polymer interactions of the blends. The common feature of these works is there are chemical shift changes and/or signal broadening of the functional groups in the ^{13}C CP/MAS spectra upon blending, which are caused by the inter-polymer hydrogen-bonding

or dipolar–dipolar interactions. Such changes in spectral feature are direct evidence of intimate mixing. Measurement of T_{CH} is demonstrated to be a useful way of probing the inter-polymer interactions. In studying of poly(epichlorohydrin) (PECH)/poly(*N*-vinyl-2pyrrolidone) (PVP) blends,[23] the T_{CH} of the carbonyl carbon of PVP decreases from 0.99 ms to 0.28 ms upon blending, when the blend contains 30 wt% of PECH. This dramatic change is attributed to the inter-polymer hydrogen-bonds formed between the carbonyl groups of PVP and the α-protons of PECH, because the protons engaged in hydrogen bonds can serve as additional source of the ^{1}H–^{13}C magnetization transfer for the carbonyl carbons. Similar results are also observed in the blends of poly(hydroxyl ether of bisphenol A) (Phenoxy) with poly(ethyl oxazoline) (PEOx).[13] In the ^{13}C CP/MAS spectra of the blends, the relative intensity of the carbonyl peak of PEOx with respect to those of the other peaks of PEOx increases with increasing the content of Phenoxy, indicating the decrease of T_{CH} of the carbonyl carbon upon blending. This is also ascribed to the inter-polymer hydrogen-bonds formed between the carbonyl groups of PEOx and the hydroxyl groups of Phenoxy. For novolac/poly(ε-caprolactone)[24] and poly(vinyl chloride)/poly(*N*-vinyl pyrrolidone)[25] blends, it is interesting to find that poly(ε-caprolactone) and poly(vinyl chloride), which are semicrystalline before blending, remain to be partially crystallized, while the amorphous parts of these two polymers are intimately mixed with their counterparts.

2.2. Elongation induced phase separation

Inter-polymer hydrogen-bonding interaction is one of the driving forces that can make dissimilar polymer pair become miscible. Poly(vinyl alcohol) (PVA)/poly(acrylic-acid) (PAA) is a typical system of such kind of blends. Previous solid-sate NMR study has revealed that due to the strong inter-polymer hydrogen-bonding interaction between the hydroxyl group of PVA and the carboxyl group of PAA, molecular level miscibility of the blend is achieved. The crystalline phase of PVA can even be destroyed completely, when the molar ratio of vinyl alcohol is equal to or less than that of acrylic-acid in the blend. Recently, by employing both solid-state ^{13}C CP/MAS NMR and wide-angle X-ray diffraction, a new experimental phenomenon, which can be termed as elongation induced phase separation, was observed in the blends of PVA/PAA.[26]

Figure 12 shows the ^{13}C CP/MAS spectra of PVA, sample I and sample II, where sample I and sample II are corresponding to PVA/PAA blends with PAA contents in monomer molar of 0.27 and 0.53, respectively. Three overlapped peaks ranged from 65 ppm to 77 ppm are attributed to methine carbon of PVA and are designated to peaks 1, 2 and 3, respectively (Fig. 13). The assignment of these three methine peaks, which had been an attractive

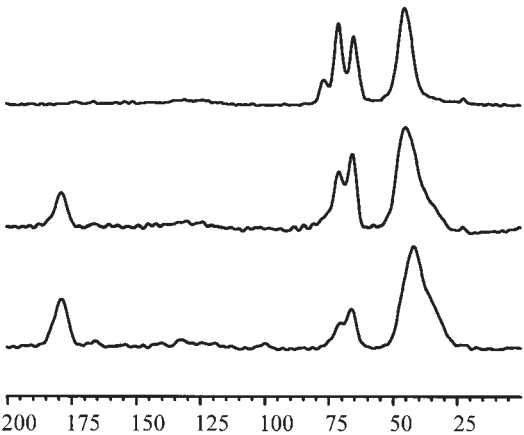

Fig. 12. ^{13}C CP/MAS spectra at room temperature: (a) PVA membrane sample; (b) sample I; (c) sample II. (Figure 1 in the original literature: Q. Chen, H. Kurosu, L. Ma and M. Matsuo, *Polymer*, 2002, **43**, 1203.)

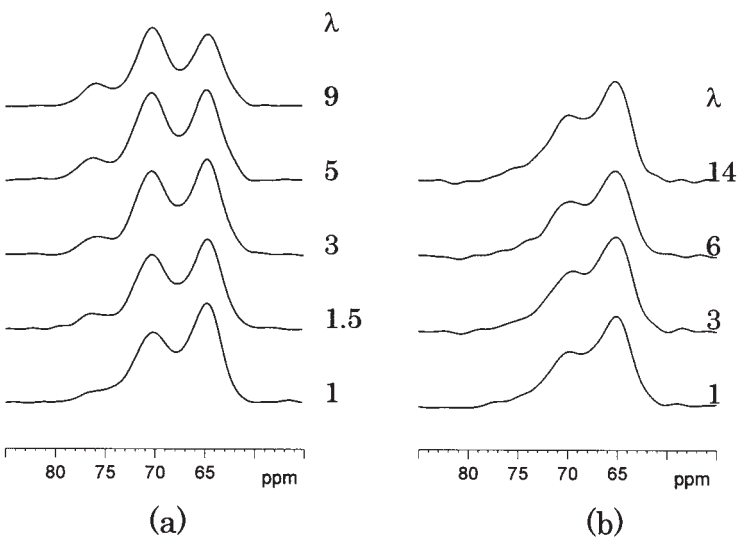

Fig. 13. ^{13}C CP/MAS spectra of the methine carbon of PVA: (a) sample I; (b) sample II with different draw ratios (λ). (Figure 2 in the original literature: Q. Chen, H. Kurosu, L. Ma and M. Matsuo, *Polymer*, 2002, **43**, 1203.)

research topic,[27,28] can be simply described as follows: Peaks 1, 2 and 3 are due to central methine carbons in triad sequences forming two, one and no hydrogen-bonds between hydroxyl groups. As is shown in Fig. 12, the relative intensities of peak 1 and peak 2 decrease with increasing PAA content, indicating the increase of the number of inter-polymer hydrogen bonds formed

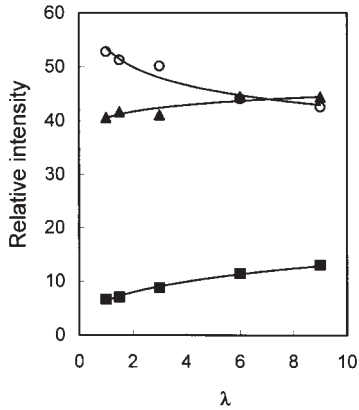

Fig. 14. Plots of the relative intensities of three methine peaks in the ^{13}C CP/MAS spectra of sample I against the draw ratio (λ), where (■), (▲) and (○) are corresponding to the data of peaks 1, 2 and 3, respectively. (Figure 3 in the original literature: Q. Chen, H. Kurosu, L. Ma and M. Matsuo, *Polymer*, 2002, **43**, 1203.)

between hydroxyl and carbonyl groups at the expense of intra-polymer hydrogen bonds formed between hydroxyl groups. This is a direct evidence of molecular level miscibility of the blends. Figure 14 shows the methine carbon signals of sample I and sample II with different draw ratios. Relative intensities of these three peaks as a function of the draw ratio are plotted in Fig. 15. From these two figures, it is evident that for sample I the relative intensity of peak 3 decreases with increasing of the draw ratio, while the relative intensities of peak 2 and peak 3 increase steadily. At the maximum draw ratio ($\lambda = 9$), the relative intensities of these three methine peaks are very close to those of the PVA membrane sample. Such a result suggests that phase separation has occurred during the elongation process. Because of the phase separation, the hydroxyl groups of PVA are able to form more intra-polymer hydrogen-bonds, as in the case of neat PVA. What is interesting is that no noticeable changes in the relative intensities of the three methine peaks with the variation of draw ratio are observed in the spectra of sample II, suggesting that the elongation induced phase separation phenomenon of PVA/PAA blends is composition dependent. Figure 4 depicts the X-ray diffraction intensity curves of sample I and sample II. The difference between the results of these two samples is obvious. The appearance of more diffraction peaks with the increase of draw ratio for sample I indicates that the degree of crystallinity increases upon elongation. This, in turn, provides further evidence for elongation induced phase separation in the sample. On the other hand, no apparent changes can be observed in the X-ray diffraction curves of sample II with increasing of draw ratio, demonstrating that PVA in the blend remains to be amorphous even at the maximum draw ratio.

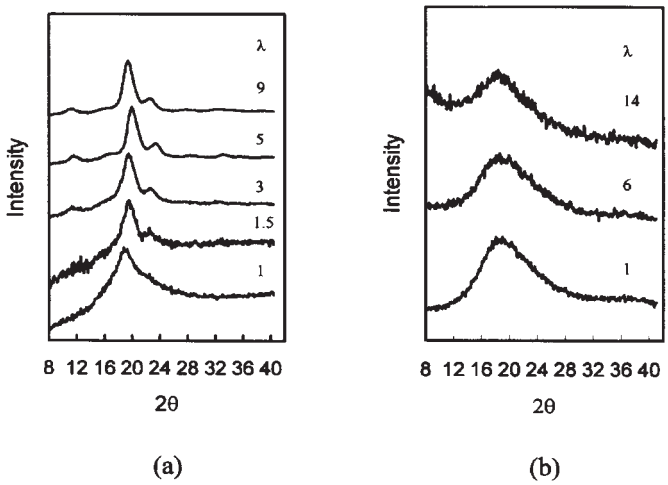

Fig. 15. X-ray diffraction intensity curves normalized to the same total intensity: (a) sample I; (b) sample II with different draw ratios (λ). (Figure 4 in the original literature: Q. Chen, H. Kurosu, L. Ma and M. Matsuo, *Polymer*, 2002, **43**, 1203.)

It is apparent that the results of X-ray diffraction agree with those obtained from NMR study.

In order to further testify the aforementioned conclusions, $T_{1\rho}{}^{H}$s of the drawn and undrawn blend samples were measured by employing ^{13}C CP/MAS method. It is found that for samples I and II before elongation, $T_{1\rho}{}^{H}$s of PVA and PAA are very close to each other, demonstrating both of them are miscible blends. However, upon elongation, the behaviour of these two samples becomes different. For sample II, the difference between the $T_{1\rho}{}^{H}$s of PVA and PAA is still within experimental error; while for sample I, marked difference can be observed. This means that for sample I upon elongation, PVA and PAA are no longer miscible on a scale of 2–3 nm. The results of $T_{1\rho}{}^{H}$ measurements, on the other hand, provide direct support to the conclusion that phase separation does happen in PVA/PAA blends with certain composition upon elongation.

2.3. Spin diffusion

Direct ^{1}H spin-diffusion measurements have been demonstrated to be a powerful tool for probing the domain size and the structural heterogeneity of multiphase polymers, including polymer blends.[29,30] These experiments normally consist of three steps: the first step is a selection period for generating an initial polarization gradient between different phase components. The second step is corresponding to a mixing time, τ_m, during which

diffusion of magnetization through dipolar interactions equilibrates the distribution of polarization. In the third step, the distribution state of polarization after τ_m is read out. By analyzing the evolution of polarization distribution with τ_m, quantitative determination of the domain size and evaluation of the degree of heterogeneity can be made.

The initial polarization gradient between different phase components can be generated by utilizing either the difference in mobility or the difference in structures of individual phase components. The mobility difference at experimental temperature can lead to difference in relaxation times like ^1H T_2, $T_{1\rho}{}^H$ etc. The differences in relaxation times can then be employed to selectively suppress the magnetization of the phase component with shorter relaxation time, while retaining the magnetization of the component with longer one. The selection of magnetization by traditional Goldman-Shen and 'dipolar filter' pulse sequences,[31,32] which are most commonly used in spin-diffusion experiments, are all based on differences in ^1H T_2 of the components. On the other hand, in ^1H solid-state high-resolution spectrum acquired by techniques like CRAMPS, signals due to different structures can be selectively suppressed or inverted.[33,34] Then the initial polarization gradient between different phase components can also be created. The read-out step of the spin-diffusion experiments can be fulfilled by directly analyzing the ^1H lineshape[35] or by indirectly monitoring the ^{13}C signal intensity changes via cross-polarization.[36]

As reviewed in the previous section, measurements of $T_1{}^H$ and $T_{1\rho}$ can provide an estimation of the length scale of miscibility of polymer blends. Compared with such kinds of experiments, the results of the spin-diffusion experiments are more quantitative and straightforward. The accuracy of the results of spin-diffusion experiments relies, to a large extent, on the values of spin-diffusion coefficients (D) employed in calculation of the constituent phase components. Despite efforts that have been made,[37] there still lacks a suitably applicable method of directly measuring the spin-diffusion coefficients, at least for polymers. For rigid polymer below T_g, 0.8 nm^2/ms has been turned out to be a reliable value of spin-diffusion coefficient.[38] The difficulty left then concerns how to determine the coefficient of the mobile phase, which is very sample dependent. Recently, through studies on diblock copolymers and blend samples with known domain sizes, Mellinger *et al.*[39] established empirical relations between the ^1H T_2 and D as follows:

$$D = (8.2 \times 10^{-6}\, T_2^{-1.5} + 0.007)\ \mathrm{nm^2/s} \quad \text{for } 0 < T_2^{-1} < 1000\ \mathrm{Hz}$$

and

$$D = (4.4 \times 10^{-4}\ T_2^{-1} + 0.26)\ \mathrm{nm^2/s} \quad \text{for } 1000 < T_2^{-1} < 3500\ \mathrm{Hz} \qquad (3.1)$$

The ^{1}H T_2 of the mobile phase is determined by a Carr-Purcell-Meiboom-Gill (CPMG) pulse sequence in that work. Based on an easily accessible NMR parameter, i.e., ^{1}H T_2, the above empirical correlation, which is claimed by the authors to be sample independent, gives a practical way to estimate the ^{1}H spin-diffusion coefficient of the mobile phase of a multiphase system and should be applicable to future studies on polymer blends either by relaxation times or direct ^{1}H spin-diffusion measurements.

In recent years, the investigation of the miscibility and heterogeneity of polymer blends by ^{1}H spin-diffusion continues to be a field of active research. Jack *et al.*[40] measured the domain sizes of compatibilized Polystyrene-(Ethylene-Propylene Rubber) blends by experiments of ^{1}H spin-diffusion. What is worth while to mention is that the domain sizes of the blend samples studied in the work are about one order of magnitude larger than those which are thought to be suitable for ^{1}H spin-diffusion measurement. This is evident by the fact that T_1^H relaxation times of polystyrene (PS) and Ethylene-Propylene Rubber (EPR), which are inherently quite different from each other, are not significantly altered upon blending. Therefore, one purpose of the work is to investigate the applicability of ^{1}H spin-diffusion measurement for studying the domain structure of immiscible blends. The selection step of the ^{1}H spin-diffusion experiments is fulfilled by employing the dipolar filter pulse sequences and the spin-diffusion process is monitored indirectly by observing the ^{13}C signals. Due to the large domain size of EPR, only a very limited amount of inter-domain spin-diffusion is observed during a mixing time of 300 ms. However, by using the 'initial rate approximation',[29] the average sizes of the dispersed EPR particles in blends can still be estimated. Because the agreement between the average domain sizes measured by NMR and SEM is poor, the authors concluded that quantitatively the NMR method employed in the work is not suitable to determine the average sizes of domains that are great than a few hundreds of nanometers. On the other hand, because the reduction tendency in the average EPR particle size upon addition of compatibilizer is reflected by the results of NMR, it is suggested that ^{1}H spin-diffusion method is qualitatively applicable for studying the domain structures of immiscible blends.

Study on the blends of ethylene-propylene-diene terpolymer (EPDM) and atactic polypropylene (aPP) reported by Silva *et al.*,[41] is another case of immiscible blends investigated by ^{1}H spin-diffusion. For a 50/50 blend, T_1^Hs of EPDM and aPP are found to be 300 and 700 ms, respectively, indicating the blends are clearly a phase-separated system. The WISE pulse sequence,[29] which is usually employed to monitor the ^{1}H spin-diffusion process in a 2D manner, is used in an alternative way: After the first $\pi/2$ pulse, the magnetization is allowed to dephase for 40 μs. During this period, the polarization of aPP is destroyed, while most of the EPDM polarization is still remained. The second $\pi/2$ pulse flips the remaining magnetization back to z direction to allow T_1^H relaxation to occur in a period of τ_m. It is apparent

that the starting points of T_1^H relaxation for EPDM and aPP are quite different from each other. The recovered polarization is finally read out via the ^{13}C signal. By doing so, the T_1^H relaxation curves of both polymers are obtained. It is found that the relaxation curve of aPP consists of two relaxation components. One is related to the original T_1^H relaxation. The additional relaxation which corresponds to a time constant of about 170 ms, is attributed to inter-domain spin-diffusion. The domain size of aPP is then estimated to be 13 nm. The above work demonstrates that for immiscible blends, the impact of inter-domain spin-diffusion, which is not observable in standard T_1^H relaxation measurement, can possibly be revealed by employing the WISE pulse sequence with suitable initial conditions. A similar idea is used by Ricardo *et al.*[42] in the study of Blends of natural rubber (NR) and polyurethane (PU). Because the constituent polymers exhibit different values of T_1^H, the blends are immiscible from point of view of NMR. By employing the standard Goldman-Shen pulse sequence to detect T_1^H relaxation of the blend, a small degree of spin-diffusion between NR and the hard segment of PU is observed.

For polymer blends constituted by a semicrystalline polymer, the miscibility study often becomes even complicated, due to the existence of one or two additional crystalline domains. Harris *et al.*[43] reported a NMR investigation on sodium poly(α-L-glutamate)/Poly(ethylene oxide) blend. The blends consist of one crystalline poly(ethylene oxide) (PEO) domain, one amorphous PEO domain, which is rather mobile, and one rigid sodium poly(α-L-glutamate) (PGNa) domain. The comparative study between PEO/PGNa blends and neat PEO by ^{13}C CP/MAS NMR and double quantum NMR spectroscopy indicates that the PEO crystallites are undisturbed upon blending. ^1H spin-diffusion measurement by a standard Goldman-Shen pulse sequence with ^{13}C detection demonstrates proximity of amorphous PEO and PGNa on a 10 nm scale.

Brus *et al.*[44] reported a solid-state NMR study on the blends of polycarbonate (PC) and PEO. Because both constituent polymers are semicrystalline, complicated domain models need to be considered. Figure 16 shows the 2D exchange ^1H NMR spectra of the 1:1 PC-PEO blend measured at different mixing times. The pulse sequence used is proposed by Caravatti *et al.*[45] and based on the CRAMPS (combination of rotation and multiple-pulse spectroscopy) technique. The diagonal peaks are, from left to right, corresponding to aromatic protons of PC, methylene protons of PEO and methyl protons of PC, respectively. As is evident by the figure, the cross-peaks indicating spin-diffusion between methylene proton of PEO and both type protons of PC become perceptible in the spectrum of 300 μs mixing time. This indicates the smallest distance between amorphous PC and amorphous PEO is about 0.5–0.6 nm. In order to evaluating the domain sizes quantitatively, WISE experiments are carried out. The spin-diffusion curves indicate that for 1:1 and 1:4 PC-PEO blends, there exist two spin-diffusion

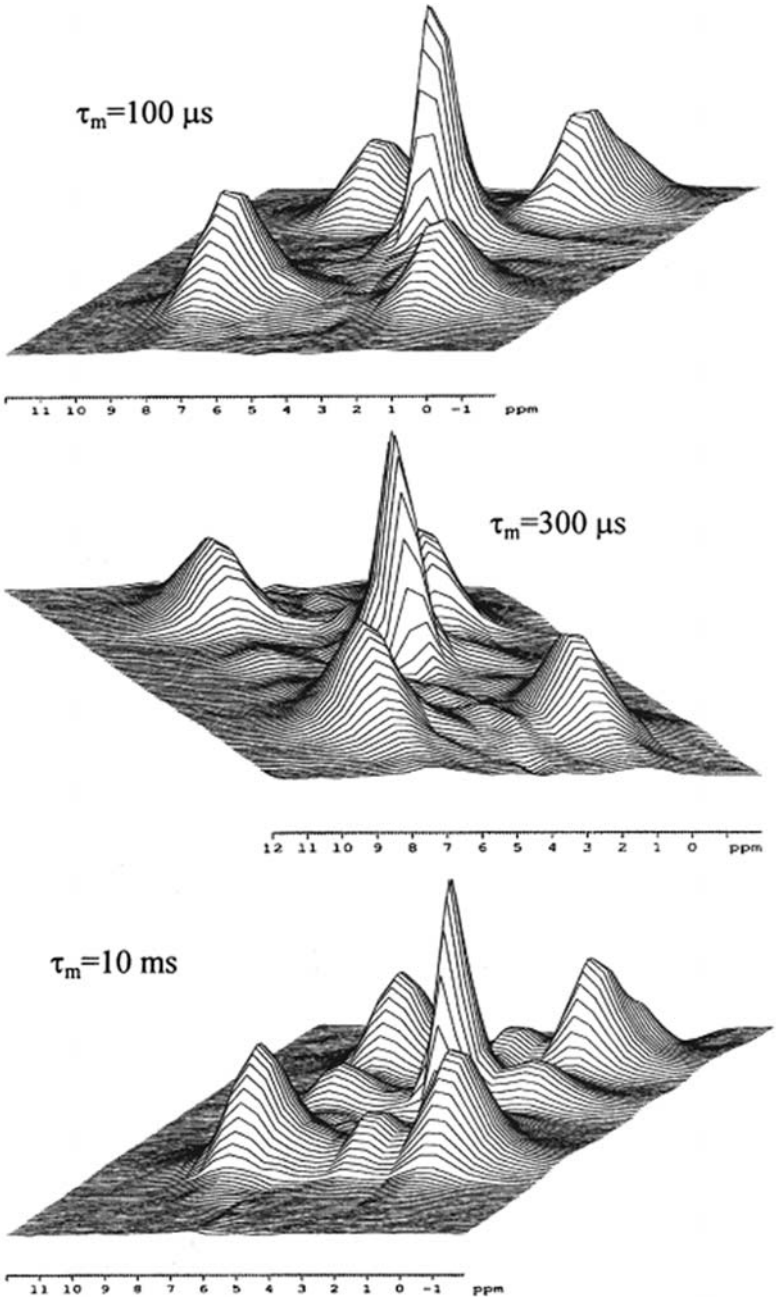

Fig. 16. 2D ^{1}H exchange NMR spectra (CRAMPS, BR24) of the 1:1 PC-PEO blend measured at different mixing times τ_m. (Figure 11 in the original literature: F. M. Mulder, W. Heinen, M. van Duin, J. Lugtenburg and H. J. M. de Groot, *Macromolecules*, 2000, **33**, 5544.)

processes. The first process corresponds to a fast magnetization transfer form mobile amorphous PEO to adjacent PC. The second slow process is due to the spin-diffusion started from amorphous PEO to crystalline PEO domain and finally to a part of PC which is assumed to be located in the inter-lamellar region of PEO. The domain model is therefore rather complicated. Numeric simulation is carried out to evaluate the spin-diffusion curves. The domain sizes and the morphology are then determined.

Mulder *et al.*[46] have studied the microscopic dynamic properties of the blends of Poly(methyl methacrylate) (PMMA) and a rubbery epoxy resin (PPO) with poly(propylene oxide) backbone. The NMR techniques involved are the standard Goldman-Shen experiment with ^{13}C detection and the WISE experiment. For the blend containing 50% PPO, the mobile domain size determined by ^{1}H spin-diffusion experiment is found to be larger than the PPO domain sizes determined by TEM. Such a result suggests that a part of PMMA is mobile in the material. As is expected, in the 2D WISE spectrum with zero spin-diffusion time, the ^{13}C signals of PPO are correlated with narrow ^{1}H lines and a very little amount ($< 5\%$) of a broader signal. This result indicates that at least 95% of the PPO polymer chains are mobile. The ^{13}C signals of PMMA, on the other hand, correlate with both broad and narrow ^{1}H lines, demonstrating further that a part of PMMA is mobile. In the 2D wise spectrum with a spin-diffusion time of 50 ms, the lineshape of PPO signals are hardly changed. This shows that during the spin-diffusion time of 50 ms, the polarization transfer between the rigid PMMA phase and the mobile PPO phase is very small. However, the lineshape of PMMA signals changed greatly. The ^{13}C signals of PMMA are now correlated with a strong narrow ^{1}H line, while the contribution of the broad component is greatly reduced. This suggests that ^{1}H spin-diffusion has equilibrated the polarization of the mobile and rigid PMMA within 50 ms, which suggests that the mobile part and the rigid part of PMMA are intimately associated. The mobile part of PMMA is estimated to be at least 40%. From the above experimental results, one interesting conclusion is drawn that the mobility of PMMA is largely enhanced at the low-frequency region by the microscopic morphology of the blend. The authors pointed out that such kind of mobility enhancement is in line with the depression of glass temperature in thin polymer films, which is a hot topic in the field of polymer physics in recent years.

By employing solid-state ^{1}H NMR techniques with fast magic-angle spinning, Mirau and Yang[47] studied the structure and dynamics of block and random ethylene oxide/propylene oxide copolymers and their composites with poly(methyl silsesquioxane). It is demonstrated that for the block copolymer embedded in the matrix of poly(methyl silsesquioxane), the segment of ethylene oxide becomes amorphous and mobile, although it is highly crystallized before blending. ^{1}H spin-diffusion measurement with a dipolar-filter pulse sequence is then carried out to determine the domain size

of copolymers in the composites. The domain sizes of block and random copolymers embedded in the composites are 4.8 nm and 7.3 nm, respectively. The NMR results, thereofore, show that the composites are very promising as ultralow-k dielectric materials. It is worth while to note that in order to avoid the possible influence of magic-angle spinning on the spin-diffusion coefficients, the ^{1}H spin-diffusion experiments are carried out in the static state.

A common feature of the above spin-diffusion experiments is to use the difference in relaxation times of the constituent polymers to create polarization gradient as the starting point of spin-diffusion. To do so, it is necessary that the constituent polymers have distinct difference in their mobility at the experimental temperatures. Mulder *et al.*[48] reported a ^{1}H spin-diffusion study on the cross-linking induced phase separation in SAN/SMA semi-interpenetrating networks, where SAN is a copolymer of styrene and acrylonitrile and SMA is a copolymer of styrene and maleic anhydride. Both copolymers are rigid at room temperature. It is therefore not possible to create a polarization gradient by utilizing the difference in ^{1}H relaxation times of the constituents. Instead of using ^{1}H CRAMPS spectroscopy, the authors employed the CP^{3} NMR spin-diffusion technique.[49] For this purpose, SAN is ^{13}C-enriched to 98% at the CN position and SMA is enriched to 98% at the CO and CH_2 positions. Figure 17 illustrates the 2D version and the 1D versions of CP3 pulse sequence. Both pulse sequences consist of three stages of CP. After the first polarization transfer from ^{1}H, ^{13}C magnetization is allowed to evolution in the period of t_1. Following a second CP transfer, the chemical shift modulated ^{13}C magnetization is transferred back to ^{1}H, and equilibration of magnetization proceeds via ^{1}H spin-diffusion. Finally, after a third CP transfer, the encoded information is detected with ^{13}C MAS NMR. As is stated by the authors, the method combines the high resolution nature of ^{13}C MAS for selection and detection with the efficient spin-diffusion via strong ^{1}H dipolar interactions. For the 1D version of the pulse sequences, a rotor synchronized DANTE pulse sequence is used to reverse the ^{13}C signal of the CN group, to create a large polarization gradient between the components. The variation of the normalized intensity of ^{13}CN signal of SAN with the spin-diffusion time t_m, is monitored, which describes the ^{1}H spin-diffusion process between components. Figure 18 shows the 2D ^{13}C–^{13}C NMR correlation spectra of the phase separated semi-interpenetrating network of SAN and SMA (50/50%; w/w) with 35% cross-linker (4,4′-methylenedianiline). For Fig. 18a, where a zero spin-diffusion time is used, strong intramolecular cross-peaks between the CO and CH_2 groups of SMA are observed, indicating that the last two CP's (totally 2 ms) are long enough for intramolecular spin-diffusion to occur. Figure 18b with a spin-diffusion time of 40 ms, shows clear intermolecular cross-peaks, demonstrating that there is a substantial inter-domain spin-diffusion. In Fig. 19, the normalized intensities of the ^{13}CN signal, acquired with the 1D version of

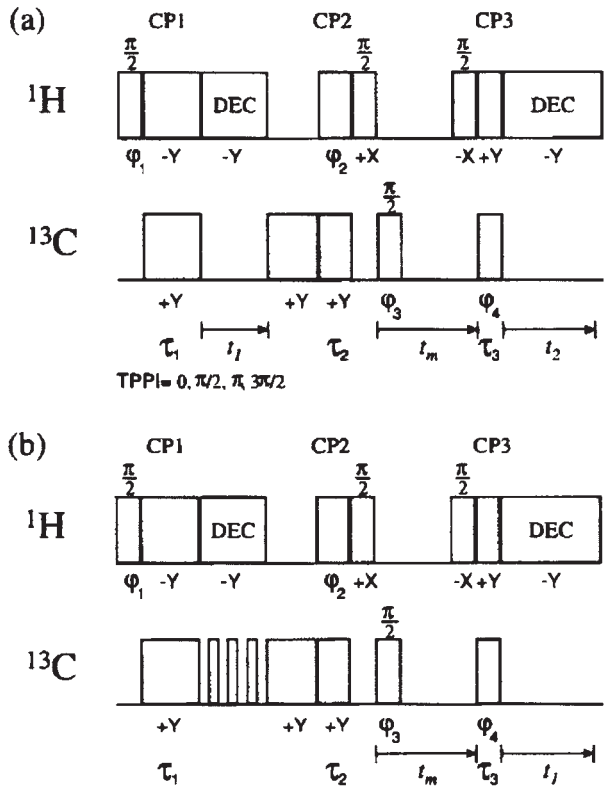

Fig. 17. CP[3] NMR pulse sequences for probing ^{1}H spin-diffusion with ^{13}C selection and detection, using 2D ^{13}C–^{13}C correlation spectroscopy (a) and using 1D inversion recovery experiment including a selective rotor-synchronized DANTE inverse period (b). (Figure 2 in the original literature: F. M. Mulder, W. Heinen, M. van Duin, J. Lugtenburg and H. J. M. de Groot, *Macromolecules*, 2000, **33**, 5544.)

the pulse sequences, are plotted against the square root of the spin-diffusion time t_m. The domain-sizes are estimated by using the standard procedures.[1] It is demonstrated that there exists a linear correlation between the domain sizes and the amount of cross-linker in SAN/SMA semi-interpenetrating network.

2.4. WISE experiments

It is known that information about the domain size, morphology and local dynamics of the blends can be obtained by 2D WISE measurements.[2950–54] The pulse sequence for the 2D WISE experiment (Fig. 20a) consists of three 90° pulses applied in the proton channel followed by a CP transfer to the

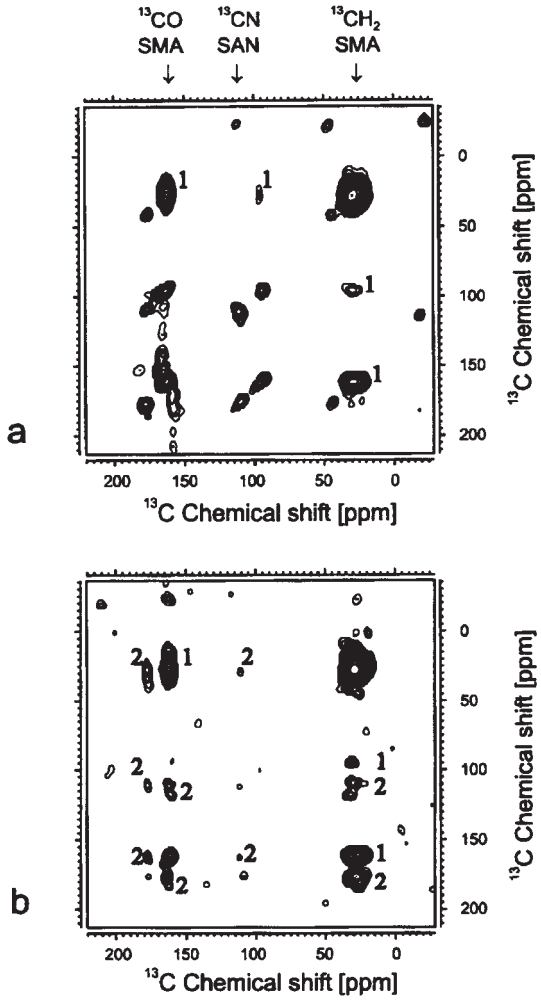

Fig. 18. 2D ^{13}C–^{13}C NMR correlation spectra of the phase separated semi-interpenetrating network of selectively ^{13}C labelled SAN and SMA (50/50; w/w) with 35% cross-linker. The measurements used duration τ_1, τ_2 and τ_3 of 2, 1, and 1 ms, respectively. The spin-lock time following t_1 was 400 μs, and the spinning speed was $\omega_r/2\pi = 6550 \pm 3$ Hz. (a) Data set collected with a mixing time $t_m = 0$ ms. The ^{13}CO and $^{13}CH_2$ of SMA resonate at 196 and 20 ppm, respectively. The correlations resulting from intramolecular magnetization exchange in SMA is indicated with **1**. (b) $t_m = 40$ ms. The ^{13}CN peak in SAN has an isotropic chemical shift of 114 ppm, with a strong sideband at 180.5 ppm that yields the more intense inter-domain correlations. They are indicated with a **2**. (Figure 3 in the original literature: F. M. Mulder, W. Heinen, M. van Duin, J. Lugtenburg and H. J. M. de Groot, *Macromolecules*, 2000, **33**, 5544.)

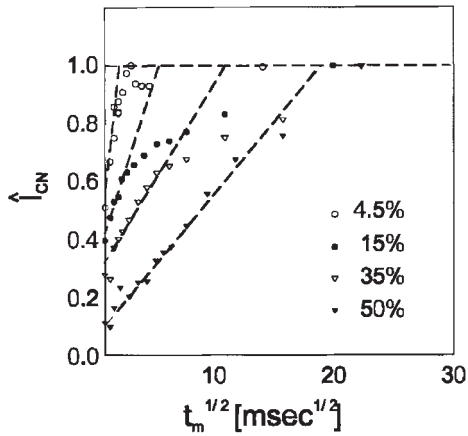

Fig. 19. Intensity $\hat{I}_{CN}$ of the CN sideband pattern of ^{13}C labelled SAN versus the square root of the mixing time t_m. The numbers indicate the amount of 4,4′-methylenedianiline cross-linker added as a percentage of the amount of MA monomers in the blend. (Figure 4 in the original literature: F. M. Mulder, W. Heinen, M. van Duin, J. Lugtenburg and H. J. M. de Groot, *Macromolecules*, 2000, **33**, 5544.)

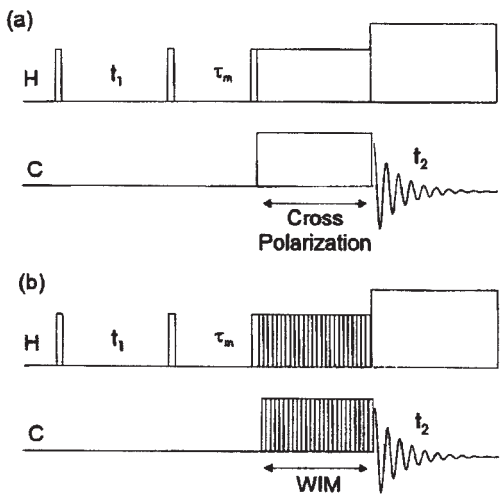

Fig. 20. The pulse sequence for 2D (a) WISE and (b) WIM/WISE NMR. t_1: ^1H evolution time, t_m: ^1H spin diffusion (mixing) time, t_2: detection time. (Figure 1 in the original literature: X. Qiu and P. A. Mirau, *J. Magn. Reson.*, 2000, **142**, 183.)

carbon system. Two-dimensional Fourier transformation yields a data matrix with the carbon frequency along one axis and the proton frequency along the other. It is typically most informative to view the data as cross sections through the 2D matrix. Since the chemical shift range for protons (5 kHz) is

much smaller than the linewidths (ca. 50 kHz), wideline spectra are observed in the t_1 dimension. Mirau *et al.* applied a modified version of 2D WISE experiment with windowless isotropic mixing (WIM) instead of CP to polystyrene (PS)/poly(vinyl methyl ether) (PVME) blend sample.[55] The pulse sequence for 2D WIM/WISE experiment is shown in Fig. 20b. The 2D WIM/WISE experiment provides an unambiguous measure of the proton dynamics because the lineshapes are not averaged by spin diffusion during the windowless isotropic mixing. The rate of spin diffusion is a factor of two less than that for the exchange of z magnetization,[29] but significant spin-diffusion can occur during the cross polarization contract times (1–2 ms) that are typically used in the solid state NMR analysis of polymers. Therefore, protons appear with a motionally narrowed lineshape in the WISE spectrum, not from molecular motion, but from spin diffusion. By using WIM instead of simple cross polarization, it can be correlated the carbon chemical shifts with the proton linewidths without the effect of spin diffusion, and the lineshapes can be related to the dynamics of individual groups in polymer chains. Figure 21 shows a contour plot of the WIM/WISE spectrum of the 50/50 molar PS/PVME blend at 27°C. The contour plot shows that very different proton linewidths are observed for the polystyrene and PVME chains, and Fig. 22 compares cross sections through the WIM/WISE spectra for the aromatic peak of polystyrene and the main chain methine peak of PVME. The aromatic protons in pure polystyrene have a full width at

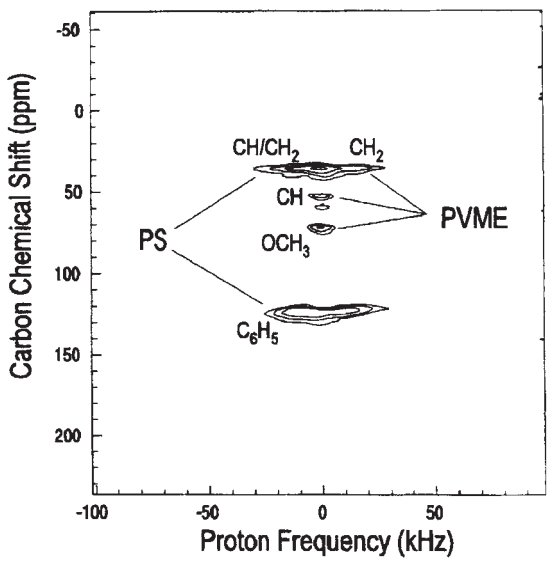

Fig. 21. A contour plot for the WIM/WISE spectrum of the polystyrene/poly(vinyl methyl ether) blend. (Figure 5 in the original literature: X. Qiu and P. A. Mirau, *J. Magn. Reson.*, 2000, **142**, 183.)

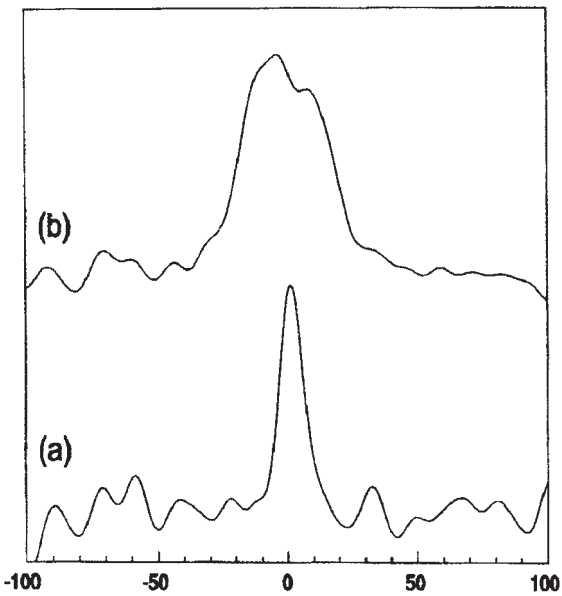

Fig. 22. Cross sections through the WIM/WISE spectrum of the polystyrene/poly(vinyl methyl ether) blend at the frequency of the (a) poly(vinyl methyl ether) methine carbon and the (b) polystyrene aromatic carbon resonance. (Figure 6 in the original literature: X. Qiu and P. A. Mirau, *J. Magn. Reson.*, 2000, **142**, 183.)

Table 6. WIM/WISE linewidths for the polystyrene aromatic protons and the poly(vinyl methyl ether) main chain methine protons as a function of temperature

Temperature (°C)	Linewidth (kHz)	
	PS C_6H_5	PVME CH
27	35.7	12.4
50	29.5	11.0
80	9.0	11.1

half maximum of 40 kHz while the same peak in the blend has a width of 36 kHz. This demonstrates that the aromatic rings are more mobile in the blend, and that they feel the effect of being dissolved in a matrix with the lower Tg PVME. The opposite effect is observed for PVME. PVME has a Tg of 31°C and chain motion at ambient temperature averages the proton lineshape to 6 kHz, WIM/WISE NMR shows that the methine motion is restricted relative to the pure PVME in the blend with polystyrene, where a 12 kHz linewidth is observed. WIM/WISE NMR has also been used to study the

effect of temperature on the chain dynamics for the PS/PVME blend, and some of the results are shown in Table 6. The polystyrene aromatic proton linewidth is reduced from 36 kHz at 27°C to 30 kHz at 50°C to 9 kHz at 80°C. By contrast, the already averaged lineshape of PVME changes to a much smaller degree over this temperature range.

REFERENCES

1. K. Takegoshi, *Annu. Rep. NMR Spectrosc.*, 1995, **30**, 97.
2. A. Asano and K. Takegoshi, *Solid State NMR of Polymers*, Chapter 10, I. Ando and T. Asakura, eds., Elsevier, Netherlands, 1998, 351.
3. S. W. Kuo and F. C. Chang, *Macromolecules*, 2001, **34**, 4089.
4. V. J. McBrierty and D. C. Douglass, *Polym. Sci., Macromol. Rev.*, 1981, **16**, 295.
5. D. E. Demco, A. Johansson and J. Tegenfeldt, *Solid State Nucl. Magn. Reson.*, 1995, **4**, 13.
6. J. Clauss and K. Schmidt-Rohr, *Acta Polym.*, 1993, **44**, 1.
7. A. Asano, M. Eguchi, M. Shimizu and T. Kurotsu, *Macromolecules*, 2003, **25**, 8819.
8. C. Lau and Y. Mi, *Polymer*, 2002, **43**, 823.
9. R.-H. Lin, E. M. Woo and J. C. Chiang, *Polymer*, 2001, **42**, 4289.
10. J. J. Dechter, *J. Polym. Sci., Polym. Lett. Ed.*, 1985, **23**, 261.
11. J. Wang, M. K. Cheung and Y. Mi, *Polymer*, 2001, **42**, 2077.
12. J. Wang, M. K. Cheung and Y. Mi, *Polymer*, 2001, **42**, 3087.
13. C. Lau, S. Zheng and Y. Mi, *Macromolecules*, 1998, **31**, 7291.
14. K. S. Jack and A. K. Whittaker, *Macromolecules*, 1997, **30**, 3560.
15. D. L. VanderHart and A. N. Garroway, *J. Chem. Phys.*, 1979, **71**, 2773.
16. P. P. Chu, J. M. Huang, H. D. Wu, C. R. Chiang and F. C. Chiang, *J. Polym. Sci. Polym. Phys. Ed.*, 1999, **37**, 1155.
17. C. De Kesel, C. Lefàvre, J. B. Nagy and C. David, *Polymer*, 1999, **40**, 1969.
18. J. Nakano, S. Kuroki, I. Ando, T. Kameda, H. Kurosu, T. Ozaki and A. Shoji, *Biopolymer*, 2000, **54**, 81.
19. H. D. Wu, C. C. Ma and F. C. Chang, *Macromol. Chem. Phys.*, 2000, **201**, 1121.
20. D. J. T. Hill, A. K. Whittaker and K. W. Wong, *Macromolecules*, 1999, **32**, 5285.
21. P. Wang and I. Ando, *J. Mol. Struct.*, 1999, **508**, 103.
22. P. Wang and I. Ando, *J. Mol. Struct.*, 1999, **508**, 97.
23. M. K. Cheung, S. X. Zheng, Y. L. Mi and Q. P. Guo, *Polymer*, 1998, **39**, 6289.
24. Z. K. Zhong, Q. P. Guo and Y. L. Mi, *Polymer*, 1998, **40**, 27.
25. S. X. Zheng, Q. P. Guo and Y. L. Mi, *J. Polym. Sci. Polym. Phys. Ed.*, 1999, **37**, 2412.
26. Q. Chen, H. Kurosu, L. Ma and M. Matsuo, *Polymer*, 2002, **43**, 1203.
27. T. Terao, S. Maeda and A. Saika, *Macromolecules*, 1983, **16**, 1535.
28. M. Kobayashi, I. Ando, T. Ishii and S. Amiya, *Macromolecules*, 1995, **28**, 6677.
29. K. Schmidt-Rohr and H. W. Spiess, *Multidimensional Solid State NMR and Polymers*, Academic Press, London, 1994 and references therein.
30. I. Ando and T. Asakura, eds., *Solid-State NMR of Polymers*, Elsevier Science, Tokyo, 1998, 351–414 and references therein.
31. M. Goldman and L. Shen, *Phys. Rev.*, 1966, **144**, 321.
32. N. Egger, K. Schmidt-Rohr, B. Blumich, W. D. Domker and B. Stapp, *J. Appl. Polym. Sci.*, 1992, **44**, 289.
33. P. Caravatti, P. Neuenschwander and R. R. Ernst, *Macromolecules*, 1986, **19**, 1889.
34. D. L. VanderHart, Y. Feng, C. C. Han and R. A. Weiss, *Macromolecules*, 2000, **33**, 2206.
35. R. A. Assink, *Macromolecules*, 1978, **11**, 1233.

36. K. Schmidt-Rohr, J. Clauss, B. Blumich and H. W. Spiess, *Magn. Reson. Chem.*, 1990, **28**, 3.
37. W. Zhang and D. G. Cory, *Phys. Rev. Lett.*, 1998, **80**, 1325.
38. J. Clauss, K. Schmidt-Rohr and H. W. Spiess, *Acta Polym.*, 1993, **44**, 1.
39. F. Mellinger, M. Wilhelm and H. W. Spiess, *Macromolecules*, 1999, **32**, 4686.
40. K. S. Jack, A. Natansohn, J. Wang, B. D. Favis and P. Cigana, *Chem. Mater.*, 1998, **10**, 1301.
41. N. M. Silva, M. I. B. Tavares and E. O. Stejskal, *Macromolecules*, 2000, **33**, 115.
42. N. M. Ricardo, M. Lahtinen, Colin Price and F. Heatley, *Polym. Int.*, 2002, **51**, 627.
43. D. J. Harris, T. J. Bonagamba and K. Schmidt-Rohr, *Macromolecules*, 2002, **35**, 5724.
44. J. Brus, J. D. Schmidt, J. Kratochvil and J. Baldrian, *Macromolecules*, 2000, **33**, 6448.
45. P. Caravatti, P. Neuenschwander and R. R. Ernst, *Macromolecules*, 1985, **18**, 119.
46. F. M. Mulder, B. J. P. Jansen, P. J. Lemstra, H. E. H. Meijer and H. J. M. de Groot, *Macromolecules*, 2000, **33**, 457.
47. P. A. Mirau and S. Yang, *Chem. Mater.*, 2002, **14**, 249.
48. F. M. Mulder, W. Heinen, M. van Duin, J. Lugtenburg and H. J. M. de Groot, *Macromolecules*, 2000, **33**, 5544.
49. F. M. Mulder, W. Heinen, M. van Duin, J. Lugtenburg and H. J. M. de Groot, *J. Am. Chem. Soc.*, 1998, **120**, 12891.
50. K. Schmidt-Rohr, J. Clauss and H. W. Spiess, *Macromolecules*, 1992, **25**, 3237.
51. N. M. da Silva, M. I. B. Tavares and E. O. Stejskal, *Macromolecules*, 2000, **33**, 115.
52. I. Quijada-Garrido, M. Wilhelm, H. W. Spiess and J. M. Barrales-Rienda, *Macromol. Chem. Phys.*, 1998, **199**, 985.
53. J. Brus, J. Dybal, P. Schmidt, J. Kratochvil and J. Baldrian, *Macromolecules*, 2000, **33**, 6448.
54. D. J. Harris, T. J. Bonagamba and J. Schmidt-Rohr, *Macromolecules*, 2002, **35**, 5724.
55. X. Qiu and P. A. Mirau, *J. Magn. Reson.*, 2000, **142**, 183.